PROCEEDINGS, Thirty-Second Workshop on Geothermal Reservoir Engineering
Stanford University, Stanford, California, January 22-24, 2007
SGP-TR-183

GEOLOGIC SETTING OF THE CHENA HOT SPRINGS GEOTHERMAL SYSTEM, ALASKA

Amanda Kolker[1], Rainer Newberry[1], Jessica Larsen[2], Paul Layer[2], and Patrick Stepp[3]

[1]Department of Geology & Geophysics, University of Alaska Fairbanks, Fairbanks, AK 99775
[2]University of Alaska Geophysical Institute, Fairbanks, AK 99775
[3]Southern Methodist University, PO Box 750395, Dallas, TX 75275
e-mail: amanda.kolker@uaf.edu

ABSTRACT

A belt of moderate-temperature geothermal activity runs east-west across central Alaska. Chena Hot Springs (CHS) is one of several Interior Alaskan hot springs in or near 55 Ma granites within Paleozoic metamorphic rocks. CHS is located within the CHS pluton, a composite body of quartz diorite, tonalite, granodiorite, and granite of both mid-Cretaceous and Early Tertiary ages. $^{40}Ar/^{39}Ar$ step heat analyses of biotite from the CHS pluton shows flat Tertiary age spectra (supporting previous studies that reported a Tertiary age for the body); however, hornblende spectra show evidence for partial resets and suggest a magmatic age of about 90 Ma. The majority of the exposed CHS pluton displays features common to Cretaceous (subduction-related) plutons elsewhere in interior Alaska. The pluton is medium to coarse-grained, commonly hornblende and allanite-bearing, with intermediate to felsic compositions and low Rb-Y-Nb-U-Th concentrations. Small bodies of mineralogically and texturally distinct syenogranite and alkali feldspar granite occur near the margins of the composite body. These rocks contain up to 8 times as much U and 4 times as much Th and Rb as the typical rocks of the CHS pluton, as is true of early Tertiary (extension-related) granites elsewhere in Interior Alaska. DIGHEM airborne gamma ray surveys indicate that high U-Th anomalies spatially correlate with outcrops of these chemically distinct granites. Thus, we propose that most of the exposed CHS pluton is Cretaceous and is underlain by an U,Th-enriched Tertiary pluton with limited surface extent. This hypothetical body reset the argon isotopic systematics of biotite and partially reset the hornblende. We further propose that radioactive decay of K, U and Th within the concealed Tertiary pluton is causing an anomalously high regional geothermal gradient, thereby providing the heat at CHS. The hydrothermal upwelling zone may occur at a fault zone junction and/or at the hypothetical contact between Cretaceous and Tertiary plutons.

INTRODUCTION AND REGIONAL GEOLOGY

Chena Hot Springs (CHS) is one of several Interior Alaskan hot springs that form a diffuse belt of moderate-temperature geothermal activity across central Alaska. The belt runs from the Seward Peninsula to the Yukon Territory. The heat source driving the geothermal activity in Interior Alaska has not been established. However, all of the hot springs are in or near granite plutons of early Tertiary age. Further, many of the hosting plutons are known to contain anomalously high concentrations of radioactive elements U and Th (Reed & Miller, 1980; Newberry, 2000). The CHS hot waters contain highly anomalous concentrations of F, B, and Li (Thermochem, 2005).

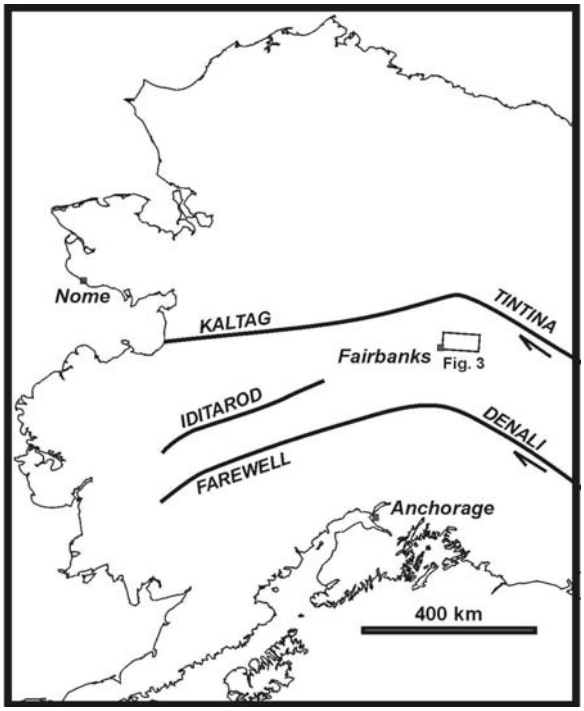

Figure 1. Location map for the CHS area in 'mainland' Alaska.

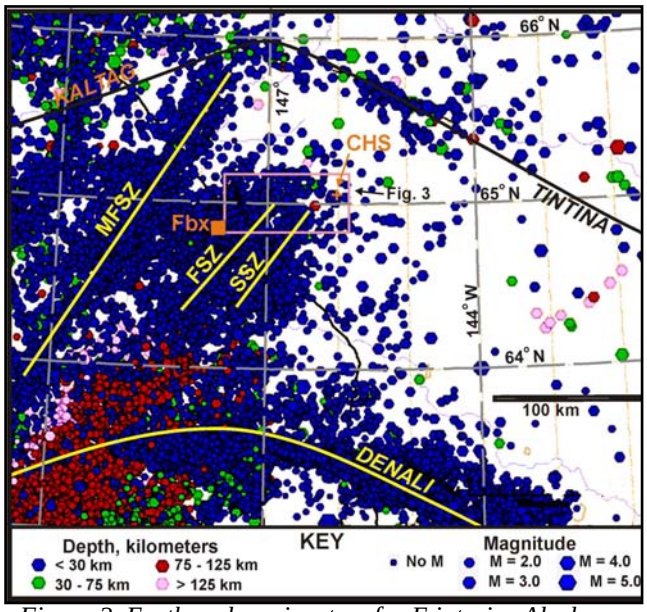

Figure 2. Earthquake epicenters for E interior Alaska recorded for the period 1996-2006.

Interior Alaska is structurally bound between two major, active, strike-slip fault systems (Figs. 1, 2) and contains numerous NE-trending zones of broadly distributed seismicity (Ratchkovski & Hansen, 2002). Due to the limited distribution of seismic stations, epicenters are not well located outside of the major road corridors. Three major NNE trending zones have been identified: Minto Flats (MFSZ), Fairbanks (FSZ), and Salcha (SSZ) seismic zones (Fig. 2).

No single fault has been identified as the source of the FSZ (Fig. 3), but rather a network of NE-trending, high-angle faults with sinistral and normal displacements are known from detailed-scale mapping in the Fairbanks area (Newberry et al., 1986). No fault has been identified as the source of the SSZ, but only regional scale geologic maps are available for this area, as for most of Interior Alaska. Page et al (1995) suggested a block-rotation model for Interior Alaska, wherein crustal blocks rotate clockwise as a result of dextral movement on the Denali and Tintina fault systems combined with sinistral movement on the NE-trending conjugate faults. It is temping to suggest--based on the epicenter locations (Fig. 2)--that CHS lies on a major NE-trending fault, however epicenters on Fig. 2 are depicted as circles 4-8 km in diameter. No faults of significance have been mapped in the CHS region (Fig. 3), based on 1:250,000 reconaissance scale mapping (Foster et al., 1983).

CHS is located near the center of a composite 5x40 km^2 pluton (Fig. 3). Biotite from a single monzogranite sample of the pluton yielded an age of 59 Ma (Biggar, 1973), conventionally accepted as the age of the CHS body. The pluton is surrounded by Paleozoic metamorphic rocks that have undergone multiple episodes of deformation and regional metamorphism and cooled to below biotite blocking temperatures by about 100 Ma (Newberry et al., 1986).

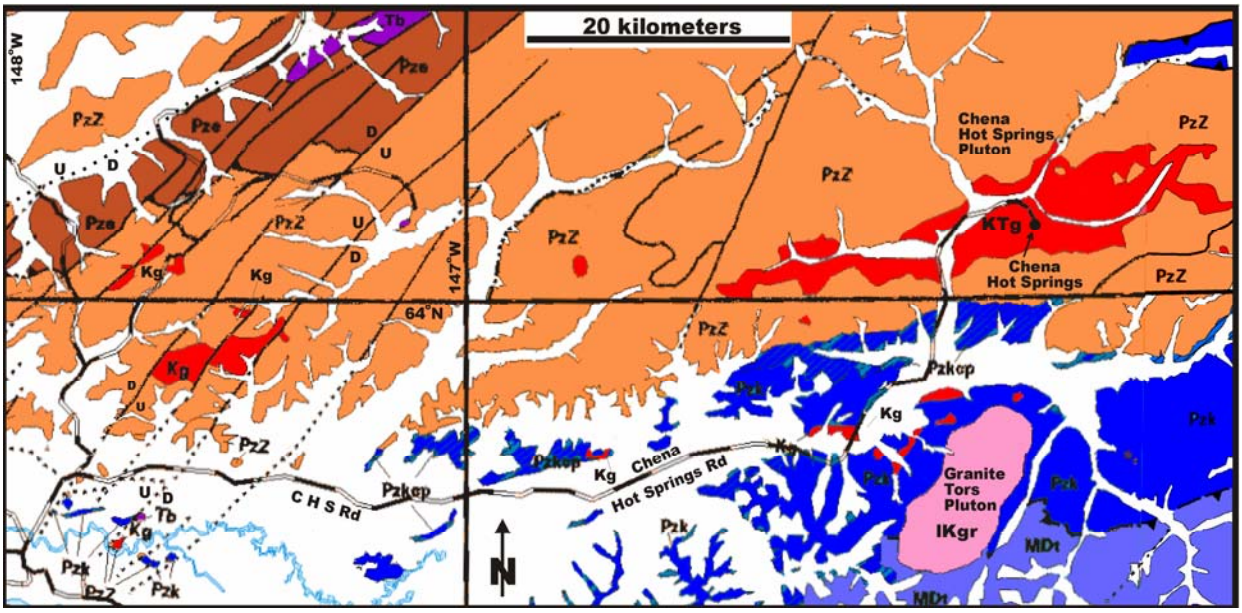

Figure 3. Generalized geologic map of CHS and vicinity; modified from Wilson et al. (1998). Key to units: white = quaternary sediments, red and pink = granitic bodies of mid-Cretaceous to early Tertiary age, purple = early Tertiary basalt, all others = metamorphic rocks (blue = greenschist, orange = epidote-amphibolite, and brown = eclogite facies).

METHODS

Field mapping focused on the plutonic rocks and major structures in the immediate Chena Hot Springs (CHS) area. Hand samples of surface rocks and cuttings from 15 geothermal wells were collected. 40 samples were thin sectioned and examined petrographically in transmitted and reflected light. Cuttings from 10-to-20-foot intervals for 11 shallow wells were examined with hand lens and binocular microscope. Cuttings from wells W1-W5 were collected from the ground next to the borehole.

For $^{40}Ar/^{39}Ar$ analysis, 6 samples were crushed, washed, sieved, and hand picked for datable mineral phases. Three samples had biotite only, while the other three had biotite and hornblende. The samples were irradiated in an uranium enriched research reactor for 20 megawatt-hours, fused, and heated in a step-wise fashion, using a 6-watt argon-ion laser following the technique described in Layer (2000). The samples were analyzed in a VG-3600 mass spectrometer at the Geophysical Institute, University of Alaska Fairbanks. The argon isotopes were measured following procedures outlined in McDougall and Harrison (1999). All ages are quoted to the $\pm$ 1 sigma level and calculated using the constants of Steiger and Jaeger (1977).

All samples were analyzed for major and trace elements using X-ray fluorescence spectroscopy (XRF). Samples were pulverized and prepared as standard pressed-powder pellets. The XRF analyses were performed at the University of Alaska Fairbanks using a Panalytical 4 kW Wavelength Dispersive Axios Spectrometer. Instrument conditions were: count times of 10 seconds for major elements and 40-60 seconds for trace elements, accelerating voltage of 32 kV for light elements and 60 kV for heavy elements, and beam current of 66 mA for light elements and 125 mA for heavy elements. The instrument was calibrated using Natural International Rock Standards. Precision based on replicate analyses is <1% of the amount present. Accuracy is approximately $\pm$5% for concentrations >20 ppm and $\pm$1-2% for concentrations >0.5%.

An airborne survey was carried out by Fugro, Inc. via DIGHEM (DIgital Helicopter ElectroMagnetics) and covered 937 km^2. The flight specifications used were typical of those used in Alaskan geophysical surveys and given in Pritchard (2005). The studies included radiometry (measured counts per second divided into Total, U, Th, and K components).

RESUTS

Rock types, mineralogy, and structure

While the dominant rock type in the 4 km^2 immediate CHS area is coarse-grained monzogranite, intermediate composition plutonic bodies, mafic dikes, and metamorphic xenoliths (1-100m^2) also occur. For purposes of mapping, the pluton was subdivided into lithologic units based on modal mineralogy and grain size (Fig. 5). The granite is typically coarse-grained, porphyritic (phenocrysts up to 2 cm^2in a 1-5 mm groundmass) but is occasionally fine-grained. Biotite is the only mafic mineral observed in the granite, with trace amounts of apatite, sphene, allanite, zircon, rutile, and small amounts of primary oxides. The granodiorite is invariably fine-grained and sub-equigranular (grain sizes 1-5mm). Hornblende is typically present, along with the minerals seen in the monzogranite. Granites often display graphic/myrmekitic intergrowths of quartz and feldspar. All plutonic and dike rocks display evidence of propylitic alteration, with replacement of biotite by chlorite, hornblende by chlorite+epidote, and plagioclase by epidote+calcite+sericite.

Lithologies encountered in geothermal wells were mostly plutonic rock of variable composition and texture, ranging from fine-grained granodiorite and quartz diorite to coarse-grained granite. Cuttings display variable degrees of alteration, shearing, and mineralized veins. Samples from all wells except W1, W3, TG6 and TG10 contain chlorite and epidote. A typical assemblage found in the cuttings associated with geothermal-water filled fractures includes clays, massive pyrite, an SiO_2-cemented microbreccia (quartz and feldspar clasts in a cristobalite/chalcedony/quartz matrix), and chalcedony veins with occasional black slickensides.

Microbreccias contain clasts of granite and clasts of quartz-epidote and quartz-feldspar veins. Rock from some geothermal wells contain breccia clasts inside a breccia matrix, signifying multiple episodes of brecciation (Fig. 4). These breccias are cemented by a cryptocrystalline SiO_2 matrix.

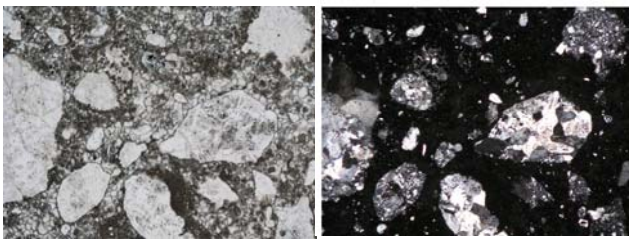

Figure 4. Photomicrographs of multiply-brecciated rock with chalcedony matrix from geothermal well W2.L: ppl; R: xpl; 1mm field of view.

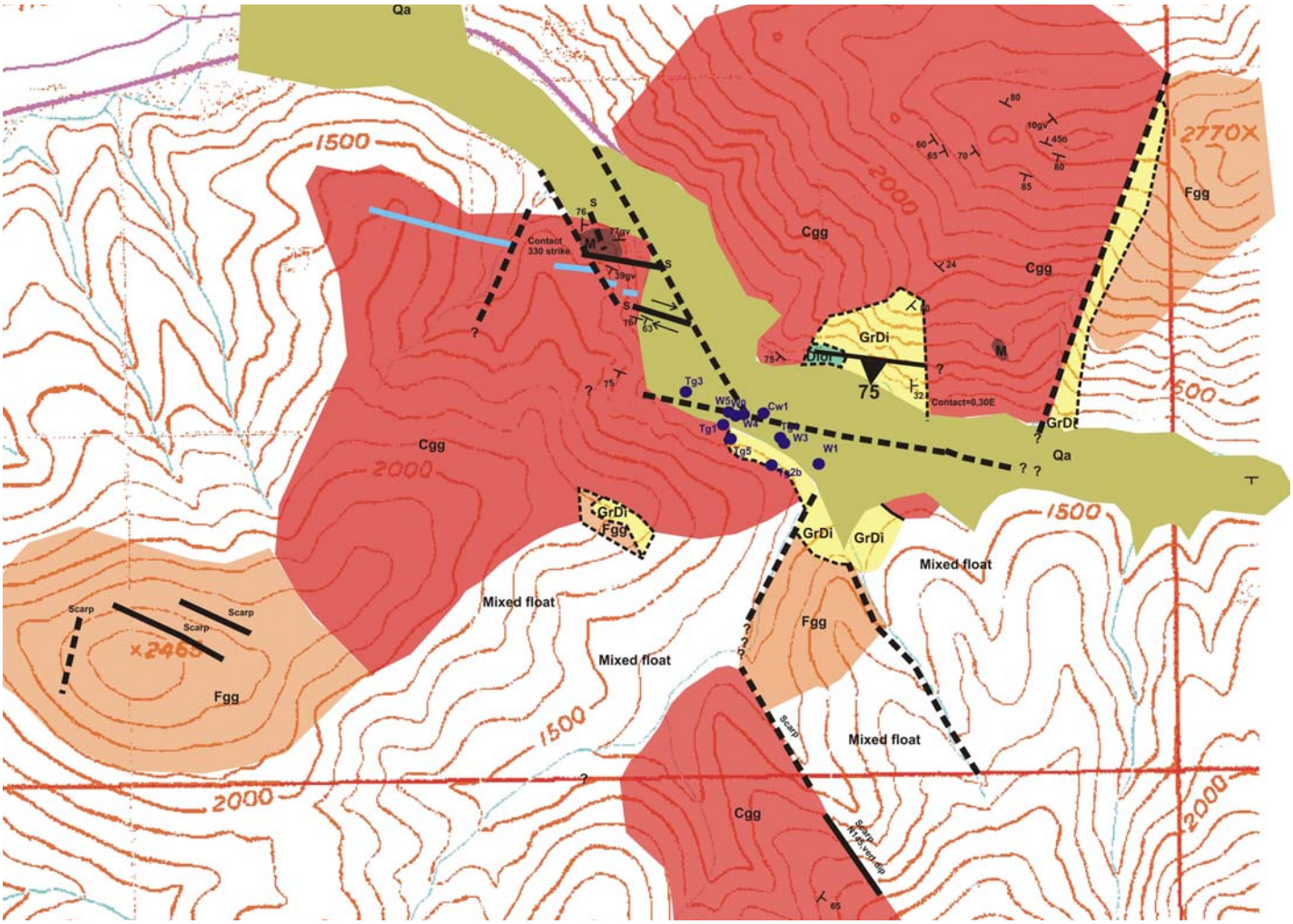

Figure 5. Geologic map of the CHS area. Key to units: beige (Qa) = quaternary alluvium; red (Cgg) = coarse grained granite; orange (Fgg) = fine grained granite; yellow (GrDi) = granodiorite and other intermediate rocks, blue = mafic dikes; brown (m) = metamorphic rocks; white = unmapped. Thick black lines = faults, dashed where inferred. Thin black lines = contacts, dashed where inferred. Blue dots = geothermal wells. Strike and dip symbols indicate joint orientations.

Chemical alteration is indicated by mineralogical replacements seen in a variety of minerals and at a variety of scales. Electron Microprobe studies both confirm the presence of allanite in the intermediate-composition plutonic rocks and its hydrothermal alteration. Allanite, a rare-earth-element (REE)-bearing epidote, occurs as a primary accessory mineral within the older units of the CHS pluton. Back-scattered electron images reveal secondary sulfide (pyrite), silicate (thoralite) and carbonate (bastnasite) minerals as alteration products (Fig. 6).

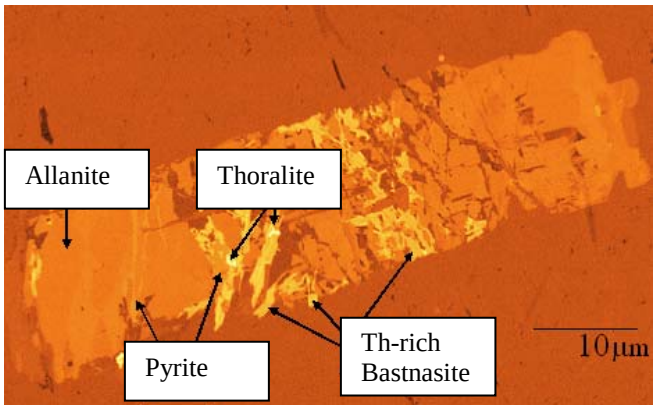

Figure 6. Back scattered electron (BSE) image of allanite in sample CHS-W4, showing various alteration minerals.

Texturally and mineralogically distinct granites occur near the pluton margin. They are highly evolved and variably associated with quartz-feldspar±tourmaline pegmatites. They are equigranular and contain tourmaline, garnet, and muscovite.

Joints, veins, and dikes in the immediate CHS area display similar orientations. The dominant orientations are approximately 100° (ESE), 130° (NW), and to a lesser extent, 20° (NNE). Joints with 100° (ESE) azimuth have an average dip of 75-85 ° S. Joints with 130° (NW) azimuth have an average dip of 65-85 SW and ~45 ° NE (Fig. 7).

Figure 7. Rose diagram showing joint orientations near CHS resort (Thorum, 2005). n=124.

While the direction of movement is unknown, slickensides on outcrop faces provide evidence for offset along a possible ESE-trending fault zone.

$^{40}Ar/^{39}Ar$ dating

$^{40}Ar/^{39}Ar$ step heat analyses of six samples yielded complex results. All six of the samples contained biotite (Table 1), three had biotite and hornblende (Table 2). All of the biotites show similar behavior, with flat plateaus for more than 80% release and less than 4% argon loss due to reset. The oldest 4 plateau ages have an average age of 60.4 ± 0.1 Ma.

Sample	Integrated Age (Ma)	Plateau Age (Ma)
008	58.8 ± 0.3	60.2 ± 0.4
030A	60.2 ± 0.3	60.4 ± 0.3
049	60.0 ± 0.3	60.6 ± 0.3
A6	58.9 ± 0.2	60.4 ± 0.2
D3	58.6 ± 0.2	59.0 ± 0.3
E6	59.3 ± 0.2	59.4 ± 0.2

Table 1. $^{40}Ar/^{39}Ar$ results for biotite grains.

Sample	Integrated Age (Ma)	Low Temp. Isochron age (Ma)	High Temp. Weighted Age (Ma)
030A	80.7 ± 0.3	60.8 ± 2.3	81.0 ± 0.7
049	74.0 ± 0.3	58.0 ± 1.1	76.7 ± 0.4
E6	78.2 ± 0.3	59.2 ± 1.4	80.3 ± 0.5

Table 2. $^{40}Ar/^{39}Ar$ results for hornblende grains.

The three hornblendes show similar, but unexpected results. The spectra consist of three distinct parts. The first, constituting the first ~10% of gas release is characterized by down-stepping ages, low Ca/K ratios and low Cl/K ratios. Isochron ages from these fractions are consistent between samples and with the biotite ages at ~60 Ma. These fractions are most likely due to biotite contamination in the hornblende. The second part of the release is characterized by Ca/K ratios that increase to a consistent value of ~5 and high Cl/K ratios (characteristics of hornblende). Ages for these fractions are the oldest, with weighted mean ages of up to 81 Ma. The last ~20% of gas release is characterized by lower Cl/K ratios, variable Ca/K ratios and younger ages, probably reflecting other inclusion mineral phases in the hornblende that do not retain argon as well as the hornblende. The original age of the hornblende is almost completely lost, but it must be older than 80 Ma.

Igneous rock compositions

To better quantify the character of the igneous rocks, major and trace element analyses were undertaken. An accepted means of converting a chemical analysis of a plutonic rock into an IUGS name is the R1-R2 method of De la Roche et al. (1980). The major element data confirm the variety of and general rock types identified in the field (Fig. 8). The bulk of the CHS pluton appears to be comprised of a uni-modal suite ranging from diorite to granite, with no obvious sharp breaks between rock types. In contrast, the tourmaline-garnet-muscovite-bearing granite from the pluton margins and the mafic dikes are chemically inconsistent. These appear to represent two different suites, perhaps two different periods of igneous activity.

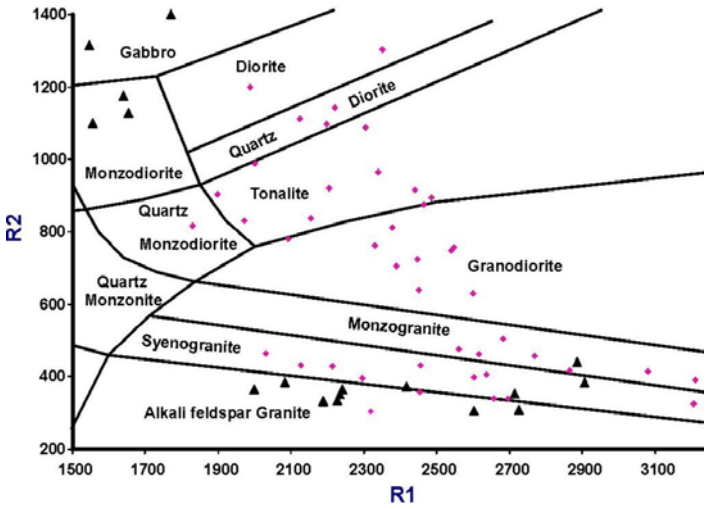

Figure 8. Rock types in the CHS pluton by major-element composition, after De la Roche et al. (1980). Diamonds = rocks from the immediate CHS area; triangles = rocks from pluton margins and mafic dikes. R1= 4Si-11(Na+K)-2(Fe+Ti); R2= Al+2Mg+ 6Ca, expressed as millication proportions.

Pearce at al (1984) distinguish between plutonic rocks of within-plate, collisional, and volcanic arc origins based on trace-element composition. In Interior Alaska, early Tertiary granites invariably

display 'within-plate' characteristics, while mid-Cretaceous granitoids show 'volcanic arc' characteristics (Newberry, 2000). Trace element composition of most CHS rocks display 'volcanic arc' characteristics (Fig. 9). The chemically distinct granites, in contrast, display compositions seen for ~55 Ma Interior Alaska granites—'within plate'.

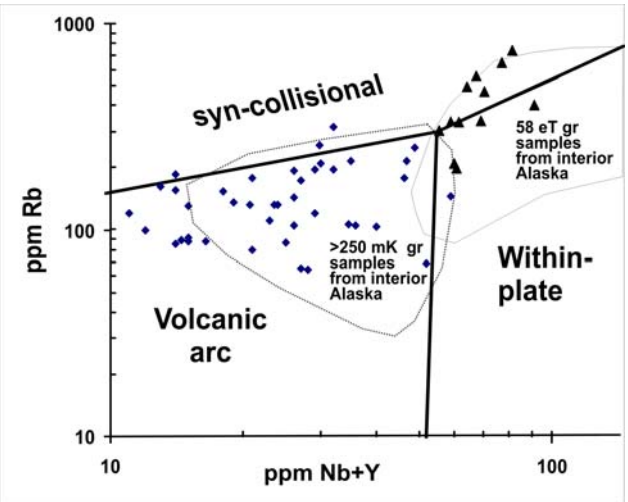

Figure 9. Granitoid discriminant diagram from Pearce et al. (1984) with data from Chena Hot springs pluton and from other mid-Cretaceous (mK) and early Tertiary (eT) granitoids from interior Alaska. CHS samples: diamonds = granite-granodiorite-tonalite with low incompatible element content; triangles = garnet-tourmaline-muscovite-biotite granite with anomalous U, Th, Sn, F, B.

The suspected early Tertiary granites have high U and Th concentrations (Fig. 10), as well as F (up to 0.3%), Sn (to 75 ppm), and Cs (to 150 ppm).

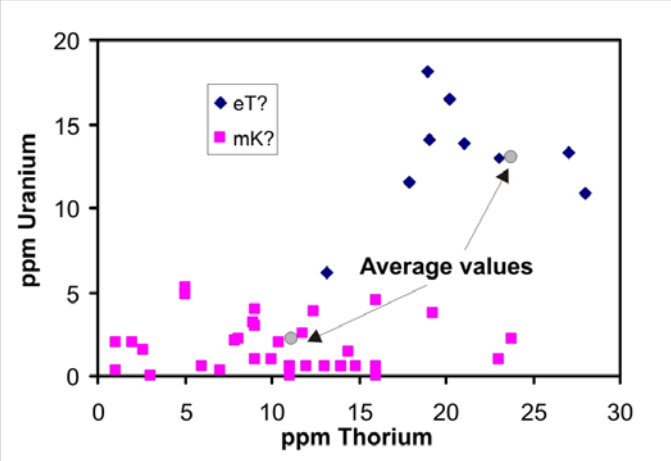

Figure 10. U and Th concentrations in rocks from CHS pluton. eT = suspected Tertiary rocks; mK = mid-Cretaceous rocks.

Mapping from airborne radiometric surveys

The airborne gamma ray survey showed anomalously high counts for U and Th (Fig. 11) primarily in the northern and eastern parts of the CHS pluton. Areas of high radioactivity correlate with outcrops of highly evolved granite. Unfortunately, variations in gamma ray counts are also due to variable soil cover, so some areas with poorly exposed U, Th-rich granite do not stand out on the radiometric maps; also, areas with well-exposed rocks of any sort will tend to yield high gamma ray counts. Based on compositional analyses from about 20 percent of the exposed pluton and the results of radiometric dating, the CHS pluton apparently contains both mid-Cretaceous and early Tertiary granitic rocks. Fig. 11 shows the approximate distribution of the two different types.

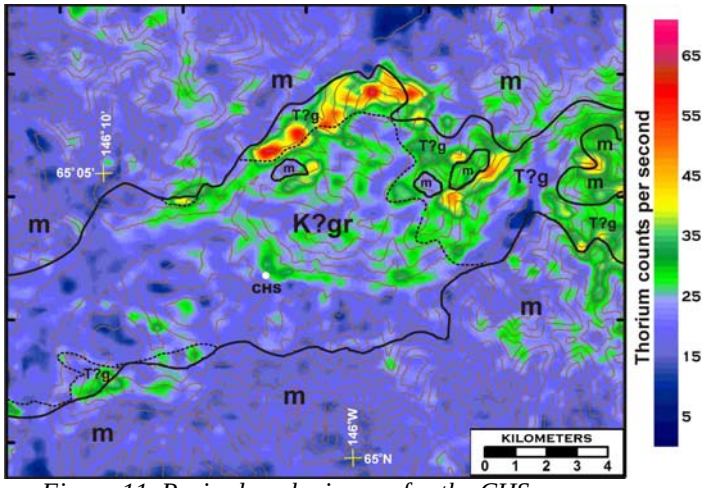

Figure 11. Revised geologic map for the CHS area. m = metamorphic rocks, K?gr = older rocks, T?g = younger granite. Modified from Foster et al. (1983), based on a combination of the radiometric maps and field traverses, 1990-2006. Topographic contour interval = 200 ft.

DISCUSSION

The surface rocks in the immediate CHS area appear to be predominantly Cretaceous, not early Tertiary as was previously reported (Biggar, 1971). Hornblende $^{40}Ar/^{39}Ar$ spectra suggest that the 60 Ma age is not the true age of the pluton, but rather represents a thermal reset age. The original age must be older than 81 Ma, and is most likely mid-Cretaceous (ca. 90 Ma). Moreover, these rocks are much more similar to other interior Alaska mid-Cretaceous than to early Tertiary plutons in terms of rock type, trace element geochemistry, and mineralogy (Figs. 6-8). The likely cause for the thermal reset is an intrusion by a very large Tertiary igneous body. Since such a body is not

obviously present at the surface, it is most likely under the exposed mid-Cretaceous pluton.

Further, the geothermal water at CHS is notably enriched in B, Li, and F, so rocks rich in these elements must be present below the surface. Enrichments in these elements are characteristic of the early Tertiary granites of Interior Alaska (Newberry, 2000). Hence, we propose that an early Tertiary granite similar to that seen at the northern and northeastern edge of the body sits below the hot springs. This body reset the K-Ar systematics in Cretaceous biotites to yield a Tertiary age.

An analogous situation occurs at Circle Hot Springs, where mid-Cretaceous and early Tertiary granitic rocks are present in a composite body. The first K-Ar date of ~70 Ma was determined from a biotite in the Cretaceous portion, ~5 km from the contact with Tertiary granite. Subsequent mapping showed compositionally different parts of the body. $^{40}Ar/^{39}Ar$ dating in the Cretaceous part yielded ages between 55 and 90 Ma, depending on proximity to Tertiary bodies (McCoy et al., 1997). The Tertiary rocks are also more enriched in U and Th than the Cretaceous rocks (Fig. 12).

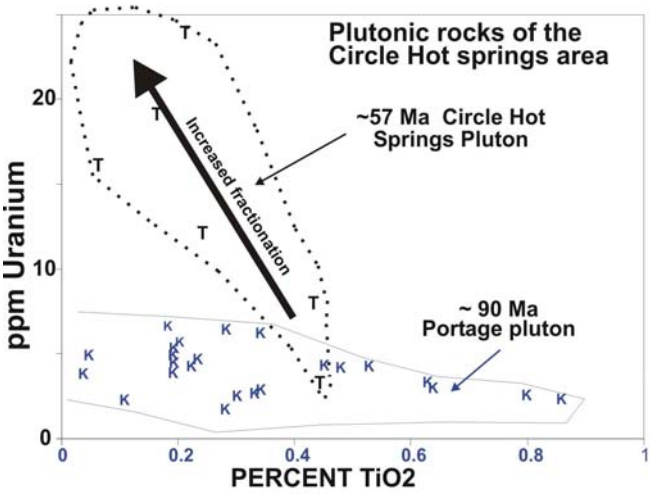

Figure 12. U concentrations in rocks from Circle Hot Springs, Alaska. Tertiary granites have significantly greater U concentrations (from Newberry et al., 2000).

Based on airborne radiometric data, U concentrations in well-exposed parts of the northern and eastern edges of the CHS pluton are approximately 3 times and Th 2-3 times as in the central part of the pluton. These count rate differences are consistent with the XRF-determined values for U and Th in the main portions and margins of the CHS pluton (see Fig. 10).

Rybach (1981) relates radioelement concentration in granitic rocks to heat production:

$$A\ (\mu W/m3) = 10^{-5}\rho\ (9.52cU + 2.56cK + 3.48cTh$$

Where

c = radioelement contencentration (U and Th in ppm, K in %)
A = heat production ρ *= rock density*

In the Tertiary granite, the average cU = 14 ppm; the average cK = 4.4%; and the average cTh = 24 ppm. Using a $\rho_{granite}$ = 2670 kg/m3, the heat production for the CHS Tertiary body is A = 6.3 μW/m3.

In addition to local elevation of the geothermal gradient by decay of elements within a concealed Tertiary pluton, the geothermal activity at CHS may also be due in part to thermal upwelling along subvertical fault planes. While no significant faults have been identified in the immediate CHS area, faulting *has* occurred at CHS. Microbrecciation in rock samples; slickensides on outcrops, inability to correlate rock types across Monument Creek; and small linear conductivity zones seen in airborne resistivity maps all indicate that faults are present. As is common for steeply-dipping faults, these postulated faults are present in major stream valleys and are not exposed at the surface. Alternatively, upwelling may be occurring at a highly fractured early Tertiary-mid-Cretaceous pluton contact.

CONCUSIONS

Radioactive decay of elements within the Tertiary pluton is one major hypothesis for explaining the heat source driving Chena and other interior hot springs. This study provides geochemical and geophysical evidence for the presence of an anomalously radioactive, younger igneous body within the CHS pluton. This body probably makes up the bulk of the subsurface rocks but is poorly exposed at the surface.

Deep groundwater circulation along subvertical fault planes may also be a factor in the geothermal activity at CHS. The junction between one major ESE-trending fault zone and another possible fault zone may be the main upwelling zone for the hydrothermal fluids. High-sensitivity seismic instrumentation was installed in December 2006 to help elucidate the question of active faulting and fault zones at CHS.

REFERENCES

Biggar, N. (1973), "A Geological and Geophysical Study of Chena Hot Springs, Alaska." Fairbanks, Alaska, *M.S. Thesis, University of Alaska.*

de la Roche, H., Leterrier, J., Grand Claude, P. and Marchal, M. (1980), "A classification of volcanic and plutonic rocks using R1-R2 diagrams and major element analyses - its relationships with current nomenclature." *Chemical Geology*, **29,** 183-210.

Foster, H.L., Laird, J., Keith, T.E.C., Cushing, G.W., and Menzie, W.D. (1983), "Preliminary geologic map of the Circle quadrangle, Alaska." *U.S. Geological Survey Open-File Report*, 83-170-A.

Layer, P.W. (2000), "Argon-40/argon-39 age of the El'gygytgyn impact event, Chukotka, Russia." Meterotics and Planetary Science, **35**, 591-599.

McCoy D, Newberry R.J., Layer P, DiMarchi JJ, Bakke A, Masterman S, Minehane DL (1997) "Plutonic-related gold deposits of Interior Alaska." In: Goldfarb RJ, Miller LD (eds) Mineral deposits of Alaska. *Economic Geology Monograph* **9**, 191-241.

McDougall, I. and Harrison, T.M., (1999), "Geochronology and Thermochronology by the $^{40}Ar/^{39}Ar$ method." New York: Oxford U. Press, 269p.

Newberry, R.J. (2000), "Mineral deposits and Associated Mesozoic and Tertiary Igneous Rocks within the Interior Alaska and adjacent Yukon portions of the 'Tintina Gold Belt': a progress report." *The Tintina Gold Belt: Concepts, Exploration, and Discoveries*, Special Vol. 2, 59-88.

Newberry, R.J., Bundtzen, T.K., Clautice, K.H., Combellick, R.A., Douglas, T., Laird, G.M., Liss, S.A., Pinney, D.S., Reifenstuhl, R.R., and Solie, D.N. (1996), "Preliminary geologic map of the Fairbanks mining district, Alaska." *Alaska Division of Geological & Geophysical Surveys*, 96-16, 2 sheets.

Page, R.A., and Plafker, G. (1995), "Block rotation in east-central Alaska: A framework for evaluating earthquake potential?" *Geology*, **23**, 629-632.

Pearce, J.A., Harris, N.B.W., and Tindle, A.G. (1984), "Trace element discrimination diagrams for the tectonic interpretation of granitic rocks." *Journal of Petrology*, **25**, 956-983.

Pritchard, R. (2005), "DIGHEM Survey for Chena Hot Springs Resort, Big Delta Quads D-4 and D-5, Circle Quads A-4 and A-5." Fugro Report #05070.

Ratchkovski, N. and Hansen, R. (2002), "New Constraints on Tectonics of Interior Alaska: Earthquake Locations, Source Mechanisms, and Stress Regime." *Bulletin of the Seismological Society of America*, **92** (3), 998-1014.

Reed, B.L.; Miller, T.P. (1980), "Uranium and thorium content of some Tertiary granitic rocks in the southern Alaska Range." *US Geological Survey Open-File Report*, OF 80-1052.

Steiger, R.H. and Jaeger, E. (1977), Subcommission on geochronology: Convention on the use of decay constants in geo and cosmochronology, *Earth and Planet Science Letters*, **36**, 359-362.

Thermochem Laboratory and Consulting Services, Santa Rosa, CA: Report of Analysis 11374-10.

Rybach, L. (1981), "Geothermal Systems, Conductive Heat Flow, Geothermal Anomalies." *In*: Rybach, L., & Muffler, L. J., Geothermal Systems, Principles and Case Histories, Wiley & Sons, 1981.

Wescott, E., & D. Turner, Eds. (1981), "A Geological and Geophysical Study of the Chena Hot Springs Geothermal Area, Alaska." *University of Alaska Geophysical Institute; Report to D.O.E.*

Wilson, F.H., Dover, J.H., Bradley, D.C., Weber, F.R., Bundtzen, T.K., and Haeussler, P.J. (1998), "Geologic Map of Central (Interior) Alaska." *U.S. Geological Survey Open-File Report*, OF 98-133.